Refining the quaternary Geomagnetic Instability Time Scale (GITS): Lava flow recordings of the Blake and Post-Blake excursions

Brad S. Singer, Herve Guillou, Brian R. Jicha, Elena Zanella, Pierre Camps

Refining the Quaternary Geomagnetic Instability Time Scale (GITS): Lava flow recordings of the Blake and Post-Blake excursions

Brad S. Singer[1], Hervé Guillou[2], Brian R. Jicha[1], Elena Zanella[3], Pierre Camps[4]

1. Department of Geoscience, University of Wisconsin-Madison, USA. bsinger@geology.wisc.edu; tel (608) 265-8650
2. Laboratoire des Sciences du Climat et de l'Environnement/IPSL, CEA-CNRS-USVQ, Gif sur Yvette, France. herve.guillou@lsce.ipsl.fr; tel : (33) 69823556
3. Universitá di Torino, Dipartimento di Scienze della Terra, Italy. elena.zanella@unito.it; tel: (39) 71339899
4. Géosciences Montpellier, CNRS and University Montpellier 2, Montpellier, France. camps@gm.univ-montp2.fr; tel: (33) 4671439 38

Abstract

The Blake excursion was among the first recognized with directional and intensity behaviour known mainly from marine sediment and Chinese loess. Age estimates for the directional shifts in sediments are poorly constrained to about 118-100 ka, i.e., at the marine isotope stage (MIS) 5e/5d boundary. Moreover, sediments at Lac du Bouchet maar, France and along the Portugese margin reveal what may be a "post-Blake" excursion at about 105-95 ka. The excursional directions are associated with a prominent paleointensity minimum between about 125 and 95 ka in global stacked records. Lava flow recordings of the Blake excursion(s) have, however, been questionable because precise ages required for correlation with these sediment records are lacking. To establish new, independent records of the Blake excursion, and link these into a larger Quaternary GITS, we have undertaken $^{40}Ar/^{39}Ar$ incremental heating and unspiked K-Ar experiments on groundmass from the transitionally magnetized Inzolfato flow on Lipari Island.

We also obtained 40Ar/39Ar incremental heating results for a lava flow on Amsterdam Island originally thought to record the Mono Lake excursion and from the transitionally magnetized El Calderon basalt flow, New Mexico that was K-Ar dated by Champion et al. (1988) at 128±66 ka. Unspiked K-Ar ages of four samples from the Inzolfato flow are 102.5±4.7, 101.3±3.3, 97.1±2.6, and 96.8±3.1 ka and thus indistinguishable from one another. 40Ar/39Ar results are more complex, with three samples yielding discordant age spectra. Based on incremental heating data obtained in both the UW-Madison and Gif-sur-Yvette 40Ar/39Ar laboratories, a fourth sample yields six concordant age plateaux and a weighted mean age of 104.9±1.3 ka that we take as the best estimate of time since the flow erupted. Five 40Ar/39Ar incremental heating experiments on the Amsterdam Island lava yield a plateau age of 121±12 ka, whereas ages from two sites in the Calderon flow are 112±23 and 101±14 ka, together giving a weighted mean of 104±12 ka. The age of 121±12 ka from Amsterdam Island, though imprecise, correlates with the Blake excursion. In contrast, the 104-105 ka age obtained from both Lipari and New Mexico indicates that these lavas record a younger period of dynamo instability, most probably associated with the post-Blake excursion. These radioisotopic ages coincide with the astronomical ages of two sharp paleointensity minima in the PISO-1500 global stack. Our findings indicate that the Blake and post-Blake excursions are both global features of past geodynamo behavior and support the hypothesis that Brunhes chron excursions are temporally clustered into two groups of a at least a half-dozen each spanning over 220 to 30 ka and 720 to 520 ka.

Introduction

Geomagnetic excursions, during which the intensity of Earth's magnetic field wanes as its direction shifts beyond secular limits for brief periods of time on the order of 10_3 y, are now widely recognized as a fundamental feature of geodynamo behavior which reflect instabilities that may also give rise to polarity reversals (Hoffman, 1981; Tric et al., 1991; Camps and Prévot, 1996; Laj and Channell, 2007; Singer et al., 2002; 2008a; Hoffman and Singer, 2008). The search for a mechanistic link between excursions and polarity reversals has led to hypotheses which consider that distinct components of the geomagnetic field may originate within specific depth domains of the outer core fluid. For example, Gubbins (1999) proposed that excursions reflect relatively rapid and short-lived (< 3 ka) reversal of the field generated by flow of liquid in the outer core, but not the solid inner core in which the field decays slowly by diffusion. Thus, only during an exceptionally long-lived excursion (>3 ka) can magnetic energy diffuse out of the inner core such that it loses control over the weakened field left in the lowermost portion of the outer core, thereby permitting polarity reversal as the dynamo re-stabilizes. More recently, Hoffman and Singer (2008) proposed that as the deeply generated axial dipole component of the geomagnetic field wanes during an excursion, a weaker and shorter wavelength, non-axial dipole field becomes dominant at Earth's surface. That this shallow core (SCOR) magnetic field source is reproduced during successive excursions and reversals is thought to reflect focusing of magnetic flux through regions of the lowermost mantle characterized by thermodynamic or electrical properties which contrast with the surrounding mantle for millions of years (Hoffman and Singer, 2008). Moreover, the frequency, timing, and morphology of short-lived excursions relative to polarity reversals provide critical observations that can help guide and interpret numerical models of outer core fluid dynamics and assess, for example, whether the dynamo is intrinsically unstable (Zhang and Gubbins, 2000), or only periodically unstable when the axial dipole is relatively weak (Singer et al., 2008a) or heat flux across the core-mantle boundary is relatively high (Glatzmaeir et al., 1999; Olson et al., 2010).

Testing these hypotheses brings an increased demand for high quality paleomagnetic data from individual excursions, new and more precise geochronologic constraints that permit correlation between sedimentary and lava flow records of excursions, and observations from sites distributed broadly across the globe (e.g., Roberts, 2008). The Geomagnetic Instability Time Scale (GITS) represents our attempt to catalogue dynamo instabilities, including excursions and polarity reversals, on the basis of $_{40}Ar/_{39}Ar$-dated lava flow recordings, Mediterranean sediment core, is complex and exhibits VGPs that transit from Northern North America to South America and back twice, with a sudden jump to Australasia during the second phase, thereby indicating at least two periods of nearly reversed polarity (Tric et al., 1991). Age estimates for the Blake excursion from sediments range from about 118 to 100 ka based mainly on comparison of the O isotope compositions of foraminifera to global Marine Isotope Stage (MIS) reference curves and indicate that it coincides with the MIS 5e/5d boundary (Table 1).

Evidence has also accumulated in support of a "post-Blake" excursion that is manifest as a period of low inclination in sediment of the Lac du Bouchet maar, France (Thouveney et al., 1990) and as an interval of relatively low paleointensity associated with a spike in cosmogenic 10Be in sediment off the Portuguese margin (Thouveny et al., 2004; Carcaillet et al., 2004) that occurs near the end of the prominent dipole low in the SINT-800 and -2000 and PISO-1500 stacks between about 105 and 95 ka (Table 1). There are at least two records in cave deposits that likely record paleomagnetic field behavior associated with the Blake excursion (Table 1). Fine-grained sediments in a cave on the

North Island of New Zealand record a directional swing toward low inclinations that occurred shortly before the deposition of flowstone that has been dated using U-Th disequilibrium at 120 ± 6 ka (Turner and Lyons (1986). A stalagmite from Cobre Cave, Spain, preserves a record of changes in paleofield direction, including two reversals during a period of apparent low field intensity, that has been dated precisely using modern 230Th isotope disequilibrium methods at between 116.5 ± 0.7 and 112.0 ± 1.9 ka (Osete et al., 2012). On the other hand, lava flow recordings of the Blake excursion are few, and these have been questionable because the precise age control required for unequivocal correlation with the sediment records is lacking (Table 1). Candidates include the transitionally magnetized Laguna basalt flow, New Mexico (Champion et al., 1988), a composite andesite flow on Lipari Island (Zanella and Laurenzi, 1998), and a pair of alkaline lava flows at Changbaishan volcano, NE China (Zhu et al., 2000). The Laguna flow that was K-Ar dated by Champion et al. (1988) at 128 ± 66 ka (2σ analytical uncertainty here and throughout the paper) is now thought to have erupted from the El Calderon vent in El Malpais National Monument (Cascadden, 1997), but it has yet to be dated using 40Ar/39Ar methods. The 40Ar/39Ar data from Lipari are complex and yield highly discordant age spectra with plateau age estimates of 157 ± 24, 143 ± 34, and 128 ± 46 ka, from two sites within the composite flow (Zanella and Laurenzi, 1998). It is also impossible to evaluate the 40Ar/39Ar age of 123±14 ka of Zhu et al. (2000) from two transitionally magnetized lava flows with very low paleointensity at Changbaishan volcano, China, as the analytical methods and supporting isotopic data were not presented, nor is it clear how the neutron fluence monitor mineral 2BH-25 is calibrated against more widely used standards. 40Ar/39Ar incremental heating experiments recently completed on samples that were collected from sites that may be equivalent to these two Changbaishan lavas at UW-Madison yield an age of 17±1 ka, thus it seems unlikely that the Blake excursion is recorded at this volcano (Singer et al., 2011). It has also been discovered that several lava flows on the Reykjanes peninsula, Iceland, previously thought to record the 41 ka Laschamp excursion, instead were erupted 94±8 ka ago and therefore reflect geodynamo behavior during the post-Blake excursion (Jicha et al., 2011).

Geologic Setting, Samples, and Geochronologic Methods
In order to firmly establish new independent records of the Blake excursion, and link these into the eomagnetic Instability Time Scale (GITS) for the Quaternary period, we have undertaken both 40Ar/39Ar incremental heating and unspiked K-Ar experiments on phenocryst free groundmass samples prepared from blocks of lava collected at five different natural outcrops within the Lo Inzolfato Formation lava studied by Zanella and Laurenzi (1998; Fig. 1). The Lo Inzolfato Formation comprises dark grey, plagioclase-phyric, glassy, high-K andesitic lava up to 50 m thick that is prominently flow-banded and oxidized in many places, and which reflects phreatomagmatic eruption of the Monte Chirica composite volcano on the northwest flank of Lipari Island (Lucchi et al., 2010). The hand specimens collected from all five sites are nearly identical in appearance, and the bulk composition of the four samples on which K-Ar measurements were made are remarkably similar, with between 3.68 and 3.89 % K (Table 2), thus we interpret the Inzolfato Formation as a single contiguous lava flow. Notably samples LP-06-01, -02, and -03 were collected within 150 m of sites G2 to G5 from which Zanella and Laurenzi (1998) obtained transitional or nearly reversed paleomagnetic directions. We have undertaken three 40Ar/39Ar incremental heating experiments on groundmass from a basaltic lava flow at sample site Am-2, from along the northwest coast of Amsterdam Island in the South Indian Ocean (Fig. 2) that was originally thought – based on very imprecise 40Ar/39Ar dating – to record a late Brunhes chron excursion, possibly the Mono Lake

excursion (Carvallo et al., 2003). From samples collected both at the site in the Calderon basalt flow, New Mexico where Champion et al. (1988) found an excursional direction, and a another site about 3 km to the northwest within the same lava from which Cascadden (1997) obtained essentially the same paleofield direction as Champion et al. (1988), we undertook six 40Ar/39Ar incremental-heating experiments.

Unspiked K-Ar procedures at Gif-sur-Yvette and intercalibration with 40Ar/39Ar results

From each of four of the samples of the Lo Inzolfato flow, approximately 200 grams was crushed and the 180-250 micron size fraction isolated for further cleaning at Gif sur Yvette. Groundmass was separated from phenocrysts of plagioclase and other phases using a Sm-Co magnet and heavy liquid, followed by hand-picking under a binocular microscope. All the samples were dated using the unspiked K-Ar technique described by Charbit et al. (1998). This technique differs from the conventional isotope dilution method in that argon extracted from the sample is measured in sequence with purified aliquots of atmospheric argon at the same working gas pressure in the mass-spectrometer. This allows mass discrimination effects between the atmospheric reference and the unknown to be suppressed, and allows amounts of radiogenic 40Ar* as small as 0.14% to be detected on a single-run basis (Scaillet et al., 2004).

The mass spectrometer sensitivity is 5.7 x 10-3 mol/A @ m/e = 40 with amplifier backgrounds of 75 x 10^{-12} A @ m/e = 40 (10^9 ohm resistor), and 5.75 10-14 A @ m/e = 36 (10^{11} ohm resistor).

The determination of K was carried out by atomic absorption with a relative precision of 1%. Argon was extracted by radio frequency heating of a 1.0 g sample in an ultra-high-vacuum glass line and purified with Ti sponge and Zr-Al getters. Isotopic analyses were performed on total 40Ar contents ranging between 2.1 10^{-11} and 5.5 x 10^{-11} mol using a 180°, 6 cm radius mass spectrometer with an accelerating potential of 620 V. The spectrometer was operated in static mode, but its volume was varied to give equal 40Ar signals for the air aliquots and the samples.

Beam sizes were measured simultaneously on a double Faraday collector in sets of 100 online acquisitions with a 1 s integration time. The atmospheric correction is monitored via two separate measurements of atmospheric argon for each sample. A first atmospheric argon aliquot (Air-1: reference dose) is measured at the same gas pressure as the sample, and serves as an isotopic reference for the determination of its radiogenic content under identical mass discrimination conditions. The second (Air-2: calibration dose) consists of a manometrically calibrated dose of atmospheric argon (from a separate reservoir of known 40Ar content). This is used to convert beam intensities into atomic abundances. As both reference aliquots (isotopic and manometric) are atmospheric in composition, they provide a cross check on the radiogenic composition of the sample. Periodic cross-calibration of zero-age standards precisely constrains the mass-discrimination to within ± 0.5‰ on the 40Ar/36Ar ratios (Scaillet et al., 2004). The manometric calibration of the Air-2 reference is based on periodic, replicate determinations of international dating standards of known K-Ar age using the same procedure for the unknowns as described in Charbit et al. (1998). This allows the total 40Ar content of the sample to be determined with a precision of about ± 0.2% (2σ). Standards used include LP-6 (127.8 ± 0.7 Ma; Odin et al., 1982, 1995) and HD-B1 (24.21 ± 0.32 Ma, (Fuhrmann et al., 1987; Hess et al., 1994; Hautmann et al., 2000). At the 95% confidence level, the values adopted here are consistent with those obtained for several 40Ar/39Ar standards through the intercalibration against biotite GA-1550 (Renne et al., 1998; Spell and McDougall, 2003). Uncertainties for the K and Ar data are 1σ analytical only, and consist of propagated and quadratically averaged experimental uncertainties arising from the K, 40Ar (total), and 40Ar* determinations. In principle, the most critical uncertainty in the K-Ar

method is that it is not possible to verify the isotopic composition of the initial argon in the sample. That is, we cannot check the assumption that, at the time of formation, the 40Ar/36Ar ratio was the modern atmospheric value (295.5). As a result, the analytical errors given in Tables 2 and 3 may be smaller than the true value.

The UW-Madison Rare Gas Geochronology Laboratory and the unspiked K-Ar laboratory at Gif-surYvette have published 40Ar/39Ar and K-Ar ages from lava samples prepared in common from the Massif Central, France that give an exceptionally precise age for the Laschamp excursion of 40.7±0.9 ka (Singer et al., 2009; including analytical and systematic uncertainties), as well as the 109±3 ka Cerro Volcán basaltic lava flow in Argentina that provides an upper limit on the timing of deposition of several glacial moraines dated using surface exposure methods (Singer et al., 2004b). Note that for dating the Laschamp excursion Singer et al. (2009) used the age of 28.201±0.046 Ma for the 40Ar/39Ar neutron fluence monitor, Fish Canyon sanidine (FCs), and the 40K decay constant of $(5.463 \pm 0.107) \times 10\text{-}10$ that were proposed by Kuiper et al. (2008).

These age determinations demonstrate that for late Pleistocene lavas which have remained closed to K and Ar, intercalibration of these two methods and laboratories can be better than ±1%. Given the interlaboratory calibration, we look to the unspiked K-Ar results for independent confirmation of the 40Ar/39Ar ages for samples that yield concordant age spectra.

40Ar/39Ar procedures at UW-Madison

From the purified groundmass separates several subsamples, 100-150 mg each, were irradiated for 60 to 120 minutes in Cu packets adjacent to either the Fish Canyon sanidine (FCs), Alder Creek sanidine (ACs), or Taylor Creek sanidine (TCs) neutron fluence standards (Renne et al., 1998) in 2.5 cm diameter Al discs. Ages have been calculated assuming the age of 28.201±0.046 Ma for FCs and 40K decay constant proposed by Kuiper et al. (2008); measurements that rely on the ACs or TCs standard have been intercalibrated to these values.

Recent experiments at UW-Madison (Singer et al., 2012) reveal that the 28.201 Ma age for FCs gives a 40Ar/39Ar age for lava flows that record the Matuyama-Brunhes reversal of 772 ka that is identical to the astronomical age for this reversal of 773 ka determined in ODP sediment cores from sites 983 and 984 (Channell et al., 2010). Correction factors for undesirable nucleogenic reactions at the Oregon State University TRIGA reactor's Cadmium-Lined In-Core Irradiation Tube (CLICIT) are based on measurements of Ca- and K-free salts, including data collected at UW-Madison, and are: [40Ar/39Ar]K = 0.00086; [36Ar/37Ar]Ca = 0.000264; [39Ar/37Ar]Ca = 0.000673 (Singer et al., 2004b). Single crystals of the FCs or four crystal aliquots of the ACs or TCs standards were fused with a 25 W CO_2 laser and their argon isotope composition was measured statically on a Balzers SEV-217 electron multiplier in analog mode; mean values from a dozen or more measurements from each Al disk were used to calculate J values. Using a resistance furnace, the groundmass subsamples were degassed at 550 ºC for 60 minutes to reduce atmospheric contamination, then incrementally heated to release the argon in 30-100º steps between 540º and 1300ºC and measured on the MAP 215-50 mass spectrometer operated at a sensitivity of 5.9 x 10-15 moles/V at UW-Madison using procedures detailed in Singer et al. (2008a). As experience with these samples grew, the gettering time after heating was extended to as long as 15 minutes to improve gas clean-up. Five or more blanks spanning the temperature range utilized were measured between each sample and were at least an order of magnitude smaller than signals from the samples. Mass discrimination was monitored by measuring the isotopic composition of atmospheric argon 6-10 times daily during each of the analytical sessions and ranged from 1.0025 to 1.0052. The variability in mass discrimination within each analytical session was less than 1-2 permil per atomic

mass unit (1σ). The ±2σ uncertainties in age include contributions from both analytical error and the intercalibrations between the FCs, ACs and TCs standards (Renne et al., 1998).

Criteria for calculating plateau ages and the isochron from the plateau data are from Singer et al. (2008a). Two to five separate incremental heating experiments comprising 6 to 12 steps each were undertaken on the Lipari and Amsterdam Island samples and where plateau criteria were met, a weighted mean plateau age was calculated from the pooled results, as well as an isochron. Because none of the experiments that yielded plateau ages are associated with an isochron which suggests that excess argon is present, and the majority of these samples turned out to be relatively poor in radiogenic argon thereby limiting spread along the isochron, we take the plateau ages as the best estimate of time since the lavas cooled below their magnetic blocking temperature. Complete 40Ar/39Ar results are in the Electronic Data Repository (Table DR1).

40Ar/39Ar procedures at Gif sur Yvette

Two incremental heating experiments were conducted on groundmass subsamples, equivalent to those on which the K-Ar data were obtained, from site LP-06-03 in the Lo Inzolfato lava flow on Lipari. Analysis was done at the new 40Ar/39Ar facility developed in our laboratory. The 130 mg samples were wrapped into 99.5% copper foil packets, loaded in aluminum disks and irradiated 45 minutes (Irradiation # 21) in the β1 tube of the OSIRIS reactor (CEA Saclay, France). The total neutron flux received by the samples ranged from 1.2×10^{14} to 2.7×10^{14} n/cm^{-2}. Neutron fluence (J) was monitored by co-irradiation of ACs crystals (Nomade et al., 2005) placed in three positions around the aluminum disk. The J value for each sample was determined from at least 8 single grain laser fusion analyses of ACs crystals. Corresponding J values were calculated using an age of 1.194 Ma (Renne et al., 1998; Nomade et al., 2005) and the total decay constants of Steiger and Jäger (1977). In turn, the ages determined at Gif-sur-Yvette were re-calibrated such that they are relative to 28.201 Ma FCs and thus comparable tothe results from UW-Madison. The J values vary by about 1% across each disk pit. Correction factors for interfering neutron reactions were determined on pure compounds (K2O, CaF2)irradiated in the same position and were: (39Ar/37Ar) Ca = 5.29×10^{-4}, (36Ar/37Ar) Ca = 3.78×10^{-4}, (40Ar/39Ar) K = 8.44×10^{-4}; (38Ar/39Ar) K = 1.57×10^{-2} (Guillou et al., 2011 and new data).

After irradiation, samples were loaded into a stainless steel carousel over a double-vacuum resistance furnace and degassed at 550 – 650°C to remove undesirably large quantities of atmospheric argon. Incremental heating experiments consisted of 8 steps between 650 and 1160°C. Each step involves 2 minutes of increase to a set-point temperature that was maintained for a total duration of 20 minutes with the gas exposed to a titanium sublimation pump. 5 Additional minutes of gas clean up were achieved by two SAES 10 GP-MK3 Zr-Ar getters operated at 400°C. The gas is then attracted for 5 minutes onto active charcoal at liquid nitrogen temperature. After attraction, this sector is isolated, and gas released at room temperature is cleaned up by an air cooled SAES C50 Zr-Ar getter operated at 250°C during another 5 minutes.

The purified gas is measured using a high-sensitivity noble gas GV5400 instrument operated in ion counting mode. One analytical run consists of 20 peak scans of each argon isotope with integration times of 1 s (40Ar, 39Ar) or 10 s (36Ar, 37Ar, 38Ar, baseline), first preceded by a peak centering routine on the five Ar isotopes, upon admission of the sample into the massspectrometer.

Raw argon isotope abundances are regressed back to inlet time using GV software (NG v.2.90) based on linear or polynomial least-squares fit. The instrument was operated at a sensitivity of 8×10^{-3} A/Torr. The precision and accuracy of the mass discrimination correction was monitored by

periodical measurements of air argon. This monitoring is performed using a dedicated air-calibration system featuring a 6-liter tank filled with purified atmospheric argon.

This tank is connected to the mass spectrometer vacuum line via two pneumatically- actuated air pipettes of approximately 0.1 and 1.0 cc. This system allows for a 1 cc (e.g. 600,000 counts s-1 (cps on 40Ar)) and a 0.1 cc (e.g. 70,000 cps on 40Ar) atmospheric aliquots to be delivered into the mass spectrometer and permits careful monitoring of the mass discrimination over a wide dynamic range with a precision better than 0.15% (2σ; standard deviation for multiple experiments) for any given beam size measured (see online supplement Fig. F1). In principle, this precision allows samples with about 1% 40Ar* or more to be measured with confidence.

System blanks were measured prior to step-heating experiments at temperatures between 600 and 1400°C. Blanks were about $1.8.10^{-16}$ mol of 40Ar and $1.0 \, 10^{-18}$ mol of 36Ar in nearly atmospheric composition. These values are about 30 to 100 times lower than the sample signals. The complete 40Ar/39Ar results are in the Electronic Data Repository (Table DR2).

Results from Lipari

Unspiked K-Ar ages for samples LP-06-02, -03, -04, and -05 from the Inzolfato flow are 103.9±4.8, 102.2±3.4, 96.8±3.1, and 97.1±2.8 ka, respectively, and are each within 2σ uncertainty of one another (Table 2). 40Ar/39Ar results are more complex, with samples from sites LP-06-04, and -05 yielding highly discordant age spectra with no meaningful plateau ages (Table 3; Fig. 3). However, the UW-Madison experiments reveal that the sample from site LP-06-03, yields a weighted mean plateau age of 105.9±2.1 ka, and this is in agreement with the unspiked K-Ar age from the same sample (Tables 2 and 3).

The two Gif-sur-Yvette experiments on sample LP-06-03 yield concordant spectra with 100% of the gas defining the age plateaus (Table 3). The 40Ar* contents range from 5.0% to 27.0%, with typical values of 15% to 25% for the plateau steps. The two plateau ages are indistinguishable from one another and the isochrons yield atmospheric intercepts. Combining the 16 plateau steps gives an age of 104.8±1.7 ka and an inverse isochron of 104.9±3.6 ka (Fig. 3). These results are within the uncertainty of those obtained from this sample at UW-Madison (Fig. 3) and the unspiked K-Ar age. We take the weighted mean of the 6 plateau ages obtained at UW-Madison and Gif-sur-Yvette, 105.2±1.4 ka (MSWD = 0.74), as the best 40Ar/39Ar age for sample LP-06-03.

Because the age spectra for all experiments on samples LP-06-04 and -05 are discordant, (Table 3; Fig. 3), we take the plateau age of 105±1 ka from sample LP-06-03, that is based on 6 separate incremental heating experiments in the two laboratories and thus 56 age-concordant gas steps, as the most precise estimate of the age of the Lo Inzolfato lava flow. Based on geologic mapping, and morphological development of the Monte Chirica volcanic vents from which this lava flowed, Lucchi et al. (2010) interpret the volcanism to be phreatomagmatic and this may explain the difficulty we encountered in obtaining a precise age from this massive, columnar jointed lava flow that contains 3.7 wt.% K2O. We suspect that a small, but pervasive component of hydrothermal- or weathering-induced alteration – enhanced owing to water vapor incorporated into the lava during its eruption – may account for the discordant age spectra in our experiments from some sites, as well as in the samples measured by Zanella and Laurenzi (1998). The Lo Inzolfato lava flow occurs between unconformities that have been linked to the sea level rise at the onset of MIS 5 ca. 124 ka, and the sea level fall corresponding to the termination of MIS 5 beginning at ca. 81 ka (Lucchi et al., 2010). Moreover, the Inzolfato flow crops out several meters above Pulera Fomation lavas which have been conventionally K-Ar dated at 104.0±3.5 ka (Lucchi et al., 2010) and several

meters below a lava flow on the upper flank of the Monte Chirica volcano that has been dated using the unspiked K-Ar method at Gif-sur-Yvette at 81±2 ka (De Rosa et al., 2003, sample LHE-05), thus our 40Ar/39Ar age of 105±1 ka is consistent with independent chronostratigraphic data.

Results from Amsterdam Island
40Ar/39Ar incremental heating experiments were conducted on groundmass separates of samples Am-1, -2, and -3, but only Am-2 yielded detectable levels of radiogenic argon in our analytical system and will be discussed here. Five incremental heating experiments on subsamples of the Am-2 groundmass yield largely concordant spectra and a weighted mean plateau age of 120±12 ka (Table 3; Fig. 3). There is no evidence of excess argon from the isochron regression of the plateau data (Fig. 3) and, because the spread along the isochron is very limited (Fig. 3), we prefer the more precise plateau age. Our 40Ar/39Ar age for the Am-2 lava differs considerably from the 18±18 ka isochron age calculated from incremental-heating data (Carvallo et al., 2003). We note that the isochron for Am-2 obtained by Carvallo et al. (2003) is associated with a 40Ar/36Ar intercept value of 288.6±1.2 which is lower than the atmospheric ratio of 295.5 and thus highly improbable for a terrestrial lava. We suspect that insufficient cleaning of the gas prior to admission to the mass spectrometer, inadequate characterization of system blanks or mass discrimination, a low ratio of sample gas relative to the blank, or some combination of all of these factors, are at the root of the imprecise, and erroneous, 40Ar/39Ar isochron ages reported by Carvallo et al. (2003).

Results from the El Calderon Flow, New Mexico
Three incremental heating experiments each were carried out on samples from two sites in the El Calderon basalt flow yielding similar results. Sample NM-10-02, from the same outcrop that the K-Ar age of Champion et al. (1988) corresponds to, yields concordant age spectra and a weighted mean plateau age of 112±23 ka. Similarly, the sample from site NM-10-03 from an outcrop equivalent to site 38 of Cascadden (1997), yields concordant age spectra and a weighted mean plateau age of 101±14 ka that is not distinguishable from that of NM-10-02 (Table 3; Fig. 3). In both cases, the 40Ar/36Ar intercepts are atmospheric in composition, but because very low radiogenic yields limit spread along the isochrons rendering them very imprecise, we take the plateau ages as the best estimate of time since eruption. The magnetic inclinations and declinations obtained from specimens at the two sites are indistinguishable (Champion et al., 1988; Cascadden, 1997), and the K/Ca ratios from the incremental heating experiments (Table 3) indicate that these sites are in the same lava flow. Accordingly, the weighted mean of the two plateau ages, 104±12 ka, is taken as the preferred age of the El Calderon basalt flow.

Implications for the age of the Blake and Post-Blake excursions and geodynamo behavior
The most detailed record of the Blake excursion from two sediment cores in the eastern Mediterranean is characterized by VGPs that transit from the north to south polar regions through the Americas twice with a sudden jump to a cluster of poles in Australasia during the second reversal (Tric et al., 1991; Fig. 4). The age model for the Tric et al. (1991) record, based on O isotope stratigraphy and tephrochronology of the two cores (Tucholka et al., 1987), suggests that the Blake excursion occurred between about 118 and 114 ka. The 40Ar/39Ar age of 120±12 ka for Amsterdam Island lava Am-2 is consistent with most age estimates for the Blake excursion, including that of Tric et al. (1991; Table 1), thus we take it to be the best radioisotopic age for the Blake excursion. If correct, this is the first well-dated record of the Blake excursion from a site in

the Southern Hemisphere. The Am-2 lava, and another adjacent lava, Am-1 (Fig. 2), are weakly magnetized and possess VGPs that fall over the Caribbean Sea (Carvallo et al., 2003), well within the path through the Americas defined by VGPs of the Tric et al. (1991) record (Fig. 4). The similarity of field behavior recorded on Amsterdam Island with that of sediment in the eastern Mediterranean appears to be consistent with the hypothesis that the Blake excursion is dominated by a large dipolar component (Tric et al., 1991). Alternatively, the clustering of VGPs over the south Atlantic Ocean and Australasia and stop-and-go behavior may reflect the decline of the axial dipole and emergence of a non-axial dipole field that originates at shallow depth within the outer core and is focused toward the surface by interactions between the lowermost mantle and outermost core fluid (e.g., Hoffman and Singer, 2008).

The 40Ar/39Ar age of 105±1 ka for the flow on Lipari Island is clearly younger than the Amsterdam Island Am-2 flow and is inconsistent with most estimates for the age of the Blake excursion (Table 1). Similarly, the 104±12 ka age from the Calderon flow in New Mexico is also younger than the Blake excursion at face value, but the large uncertainty does not preclude a correlation with other recordings of the Blake. The age of 105 ka does, however, fall within the prominent low in relative paleointensity that is recorded in Portuguese margin sediment (Thouveny et al., 2004) and globally in the SINT-2000 (Valet, et al, 2005) and PISO-1500 (Channell et al., 2009) stacks between about 105 and 95 ka. This period of low intensity is associated with a spike in cosmogenic 10Be in the Portuguese margin cores (Carcaillet et al., 2004) where it has been called the Post-Blake excursion (Thouveny et al., 2004) – owing in part to an age similar to that assigned to the directional anomaly recorded in Lac du Bouchet sediment (Thouveny et al., 1990). Alongside the recent 40Ar/39Ar and 238U/230Th dating at 94±8 ka of two transitionally magnetized lava flows at Skalamaelifell, Iceland that originally had been thought to record the Laschamp excursion (Jicha et al., 2011), the 105 ka age from Lipari and New Mexico provides the first direct radioisotopic age constraints for the Post-Blake excursion. We interpret the paleomagnetic directions associated with these lava flows to reflect field geometries that perhaps varied from site to site as the magnetic field remained unstable between 105 and 94 ka. Three VGPs from the Lo Inzolfato lava flow fall over northern Japan, whereas a fourth is in the southern Pacific Ocean (Zanella and Laurenzi, 1998; Fig. 4). The VGPs of the EL Calderon flow, and 15 lava flow sites in the Skalamaelifell area, Iceland (Jicha et al., 2011), plot over the western Pacific Ocean and may be consistent with the short-lived VGP transit and cluster over Australasia that occurs during the second portion of the earlier Blake excursion (Tric et al., 1991). This interpretation leads us to suggest either that the geometric pattern of field behavior during these successive excursions was broadly similar, or that the rough age model for the Tric et al. (1991) record is inaccurate and may actually span both the Blake and Post-Blake excursions between about 120 and 94 ka.

The Brunhes Chron GITS

Laj and Channell (2007) reviewed the paleomagnetic evidence and geochronologic data in support of excursions during the Brunhes and Matuyama chrons, concluding that adequate chronology is available for only seven excursions during the Brunhes chron, including the Mono Lake (33 ka), Laschamp (41 ka), Blake (121 ka), Iceland Basin (188), Pringle Falls (211 ka), Big Lost (560-580 ka), and Stage 17 (670 ka) excursions (Fig. 5). With the exception of the Iceland Basin and Stage 17 excursions, both O isotope-based astrochronology (Channell, 1999; 2006; Channell et al., 2004) and 40Ar/39Ar radioisotopic age constraints (Singer et al., 2002; 2008a; 2009) are available. Moreover, the Mono Lake and Laschamp excursions are also dated via correlating O isotope and paleointensity

variations in marine sediment to varve-counted ice core chronologies in which O isotopes and 10Be flux peaks have been measured (Laj et al., 2004; Singer et al., 2009). Subsequent to the Laj and Channell (2007) review, Singer et al. (2008b) reported 40Ar/39Ar ages from lava flows in the West Eifel volcanic field that record five excursions in the lower Brunhes chron at 727, 630, 583, 559, and 531 ka (re-calculated relative to 28.201 Ma FCs); four of these are newly identified, and one corresponds to the Big Lost excursion which is also recorded by lava flows in Idaho, La Palma, and Tahiti at 583 ka (Singer et al., 2002; Hoffman and Singer, 2004; Roberts 2008) (Fig. 5). In addition, Cassata et al. (2008) and Kissel et al. (2011) obtained 40Ar/39Ar ages from lava flows in New Zealand and Tenerife that record the Mono Lake excursion at 32-33 ka. Moreover, the recent 40Ar/39Ar and 238U/230Th dating of the Skalamaelifell lavas, Iceland by Jicha et al. (2011) are consistent with the results presented here and indicate that the Post-Blake excursion occurred between about 105 and 94 ka.

With the addition of the ~100 ka Post-Blake excursion, the GITS for the Brunhes chron now comprises twelve well-dated excursions (Fig. 5). Notably, ten of these excursions are recorded by lava flows that have been precisely dated using modern 40Ar/39Ar analytical methods and standards; two others are exceptionally well-expressed in in multiple ODP cores where they have been dated via astrochronology. Despite observations from sediment cores in the eastern Mediterranean Sea (Langereis et al., 1997) and at ODP site 1062 in the northeastern Atlantic Ocean (Lund et al., 1998; 2006) that as many as four excursions may have occurred between about 520 and 220 ka, none of these are directly dated by O isotope-based astrochronology, nor have we yet found an excursion recorded by a lava flow that has been dated using the 40Ar/39Ar method within this interval. Thus, the GITS for the Brunhes chron exhibits a strong degree of temporal "clustering", with two groups of a half-dozen excursions each that occur during ca. 200 ka periods between about 220 and 30 ka and 730 and 520 ka (Fig. 5). Using the PISO-1500 paleointensity stack (Channell et al., 2009), the excursions of the Brunhes chron are concentrated into periods characterized on average by slightly lower paleointensity compared to the intervening period. Upon closer inspection, the Laschamp and Iceland Basin excursion each coincide with period during which the Virtual Dipole Moment (VDM) dropped below 3x1022 Am2, whereas the Mono Lake, Pringle Falls, Blake and post-Blake excursions occurred when the virtual dipole strength was not quite as low, but far lower than average, about 4x1022 Am2 (Fig. 5). These six excursions comprise an upper Brunhes chron temporal "bundle" wherein each excursion is associated with a precipitous drop in relative paleointensity to values nearly as low as that associated with the Matuyama-Brunhes polarity reversal (Fig. 5). Given the uncertainties associated with the 40Ar/39Ar ages, it is also possible to correlate the West Eifel, Big Lost, and Stage 17 excursions in the lower Brunhes chron to intensity minima along the PISO-1500 stack during the period between about 730 and 520 ka when the intensity was on average lower than the during the subsequent 300 ka (Fig. 5). Similar to the well-dated excursions of the upper Brunhes chron, each of these lower Brunhes chron excursions can be correlated with an abrupt drop in relative paleointensity. For the Big Lost and West Eifel 5 excursions the VDM dropped below 3x1022 Am2, a level not again attained until the Iceland basin and Laschamp excursions (Fig. 5). In comparing the timing of these excursions to a paleointensity record from the sediment in the Philippine Sea, rather than the PISO-150 stack used here, Roberts (2008) also illustrated that during the middle portion of the Brunhes chron magnetic field intensity remained relatively high and did not drop below threshold values that perhaps would promote excursions.

Thus, during the Brunhes chron, the dynamo may have periodically switched, on a ca. 200-300 kyr time scale, between a state characterized as relatively weak and unstable that is prone to repeated abrupt and precipitous drops in strength of the axial dipole to one that is slightly stronger and more stable during which excursions become less likely. Results from numerical simulations of the geodynamo by Glatzmaeir et al. (1999) and Olson et al. (2010) reveal that the frequency of reversals and excursions increases when heat flux through the core-mantle boundary (CMB) is high. If correct, our Brunhes chron GITS raises the possibility that heat flux across the CMB rises and falls significantly on time scales of only a few hundred thousand years, a short term variation that may be superimposed on the far slower changes in CMB heat flow that reflect the pace at which plate-tectonics and mantle convection may induce cooling within the lowermost mantle (e.g., Hoffman and Singer, 2004).

Conclusions

The 40Ar/39Ar ages of three transitionally magnetized lava flows, permit for the first time, a precise correlation of the field behavior that they record with independent records, including global paleointensity stacks from marine sediment. The 40Ar/39Ar age of a low-K basaltic lava flow on Amsterdam Island that records excursional directions and low intensity of the geomagnetic field is 120±12 ka, thus we infer that it records the Blake excursion. In contrast, an andesitic lava flow on Lipari Island, and a low-K basaltic lava in the Zuni-Bandera volcanic field, New Mexico, that each record excursional paleofield directions, give identical 40Ar/39Ar ages of 105±1 and 104±12 ka, respectively. Agreement between 40Ar/39Ar ages obtained from one of the Lipari samples at UW-Madison and Gif-sur-Yvette is excellent and demonstrates that the two laboratories are intercalibrated to within 1% of one another for challenging late Quaternary lava flows. The lavas from Lipari and New Mexico are younger than the lava on Amsterdam Island and we propose that both record the Post-Blake excursion, although given the large uncertainty we cannot rule out that the lava in New Mexico instead records the Blake excursion. Our findings from lava flows in this study, along with the recent direct dating of transitionally magnetized lavas at Skalamaelifell, Iceland (Jicha et al., 2011), and speleothem carbonate in Spain (Osete et al., 2012) indicate that the Blake and post-Blake excursions are both global features of past geodynamo behavior and strongly support the hypothesis that twelve well dated Brunhes chron excursions are temporally clustered into two groups of a half-dozen each spanning over 220 to 30 ka and 720 to 520 ka. Moreover, the new ages of these lava flows support the hypothesis of Roberts (2008) and Channell et al. (2009) that these excursions are triggered as the axial dipole field abruptly collapses such that global magnetic field intensity falls below a critical threshold value for a brief period of no more than a few kyr and that such events were common during the Brunhes chron.

References Cited

Camps, P., Prévot, M., 1996. A statistical model of the fluctuations in the geomagnetic field from paleosecular variation to reversal. Science 273, 776-779.

Carcaillet, J., Bourlès, D.L., Thouveny, N., Arnold, M., 2004. A high resolution authigenic 10Be/9Be record of geomagnetic moment variations over the last 300 ka from sedimentary cores of the Portuguese margin. Earth Planet. Sci. Lett., 219, 397–412.

Carvallo, C., Camps, P., Ruffet, G. Henry, B., and Poidras, T., 2003. Mono Lake or Laschamp geomagnetic event recorded from lava flows in Amsterdam Island (southeastern Indian Ocean). Geophys. J. Int., 154, 767-782.

Cascadden, T.E., 1997. Quaternary volcanism in the Colorado-Plateau-Basin and Range transition zone: Zuni-Bandera and nearby volcanic fields. PhD dissertation, University of New Mexico, Albuquerque, 187 pp.

Cassata, W.S., Singer, B.S., Cassidy, J., 2008. Laschamp and Mono Lake geomagnetic excursions recorded in New Zealand. Earth Planet. Sci. Lett. 268, 76–88.

Champion, D.E., Lanphere M.A , Kuntz, M.A. 1988. Evidence for a new geomagnetic reversal from lava flows in Idaho: discussion of short polarity reversals in the Brunhes and late Matuyama polarity chrons. J. Geophys. Res. 93, 11667-11680.

Channell, J.E.T., 1999. Geomagnetic paleointensity and directional secular variation at Ocean Drilling Program (ODP) Site 984 (Bjorn Drift) since 500 ka: comparisons with ODP Site 983 (Gardar Drift). J. Geophys. Res. 104, 22,937-22,951.

Channell, J.E.T., J.H. Curtis, B.P. Flower, 2004. The Matuyama-Brunhes boundary interval (500-900 ka) in North Atlantic drift sediments. Geophys. J. Int. 158, 489-505.

Channell, J.E.T., 2006. Late Brunhes polarity excursions (Mono Lake, Laschamp, Iceland Basin and Pringle Falls) recorded at ODP Site 919 (Irminger Basin). Earth Planet. Sci. Lett., 244, 378-393.

Channell, J.E.T., Xuan, C., Hodell, D.A., 2009. Stacking paleointensity and oxygen isotope data for the last 1.5 Myr (PISO-1500). Earth Planet. Sci. Lett. 283, 14-23.

Channell, J.E.T., Hodell, D.A., Singer, B.S., Huang, C., 2010. Reconciling astrochronological and 40Ar/39Ar ages for the Matuyama-Brunhes boundary and late Matuyama Chron. Geochem. Geophys. Geosyst. doi:10.1029/2010GC003203.

Charbit, S., Guillou, H., Turpin, L., 1998. Cross calibration of K-Ar standard minerals using an unspiked Ar measurement technique. Chem. Geol. 150, 147-159.

Coe, R.S., B.S. Singer, M.S. Pringle and X. Zhao, 2004. Matuyama-Brunhes reversal and Kamikatsura event on Maui: paleomagnetic directions, 40Ar/39Ar ages and implications. Earth Planet. Sci. Lett. 222, 667-684.

Creer, K.M., P.W. Readman, and A.M. Jacobs, 1980. Paleomagnetic and paleontological dating of a Section at Gioa Tauro, Italy: identification of the Blake Event. Earth Planet. Sci. Lett. 50, 289-300.

Creer K.M., Thouveny, N., Blunk, I., 1990. Climatic and Geomagnetic influences on the Lac du Bouchet palaeomagnetic SV record through the last 110 000 years. Phys. Earth Planet. Inter. 64, 314-341.

Denham, C.R., 1976. Blake polarity episode in two cores from the Greater Antilles outer ridge. Earth Planet. Sci. Lett. 29, 422-443.

DeRosa , R., Guillou, H., Mazzuoli, R., Ventura, G., 2003. New unspiked K-Ar ages of volcanic rocks of the central and western sector of the Aeolian Islands: reconstruction of the volcanic stages. J. Volcanol. Geotherm. Res. 120, 161-178.

Glatzmaier, G.A., R.S. Coe, L. Hongre, P.H. berts, 1999. The role of Earth's Mantle in controlling the frequency of geomagnetic reversals, Nature 401, 885-890.

Gubbins, D., 1997. The distinction between geomagnetic excursions and reversals. Geophys. J. Int. 137, F1-F3.

Guillou, H, Singer, B.S., Laj, C., Kissel, C., Scaillet,S., Jicha, B., 2004. On the Age of the Laschamp geomagnetic event, Earth Planet. Sci. Lett. 227, 331-343.

Guillou, H, Nomade, S., Carracedo, J.C., Kissel, C., Laj, C., Torrado, F.J.P., Wandres, C., 2011. Effectiveness of combined unspiked K-Ar and 40Ar/39Ar dating methods in the 14C age range. Quaternary Geochronology, 6, 530-538.

Guyodo, Y., Valet, J.-P., 1999. Global changes in intensity of the Earth's magnetic field during the past 800 kyr, Nature 399, 249-252.

Hoffman, K.A., 1981. Paleomagnetic excursions, aborted reversals, and transitional fields. Nature, 294, 67-68.

Hoffman, K.A., Singer, B.S., 2004. Regionally recurrent paleomagnetic transitional fields and mantle processes. In: Channell, J.E.T., Kent, D.V., Lowrie,W., Meert, J.G. (Eds.), Timescales of the Paleomagnetic Field,. American Geophysical Union, Geophysical Monograph 145, pp. 233–243.

Hoffman, K.A., Singer, B.S., 2008. Magnetic source separation in Earth's outer core. Science, 321, 1800.

Jicha, B.R., Kristjánsson, L. Brown, M.C., Singer, B.S., Beard, B.L., Johnson, C.M., 2011. New age for the Skálamælifell excursion and identification of a global geomagnetic event in the late Brunhes chron. Earth Planet. Sci. Lett., 310, 509-517.

Kissel, C., Guillou, H., Carracedo, J.C., Nomade, S., Perez-Torrado, F., Wandres, C., 2011. The Mono Lake excursion recorded in phonolitic lavas from Tenerife (Canary Islands): Paleomagnetic analyses and coupled K/Ar and Ar/Ar dating. Phys. Earth Planet. Inter., 187, 232-244.

Laj, C., Channell, J.E.T., 2007. Geomagnetic Excursions, Treatise on Geophysics 5, 373-416.

Laj, C., Kissel, C., Beer, J., 2004. High resolution global paleointensity stack since 75 kyr (GLOPIS-75) calibrated to absolute values. In: Channell, J.E.T., Kent, D.V., Lowrie,W., Meert, J.G. (Eds.), Timescales of the Paleomagnetic Field,. American Geophysical Union, Geophysical Monograph 145, pp. 255–265.

Laughlin, A.W., Perry, F.V., Damon, P.E., Shaffiqullah, M., WoldeGabriel, G., McIntosh, W., Harrington, C.D., Wells, S.G., Drake, P.G., 1993. Geochronology of Mount Taylor, Cebollita Mesa, and Zuni-Bandera volcanic fields, Cibola County, New Mexico. New Mexico Geology 14, no. 4, 81-92.

Lucchi, F, Tranne, C.A., Rossi, P.L., 2010. Stratigraphic approach to geological mapping of the late Quaternary volcanic island of Lipari (Aeolian archipelago, southern Italy). in: Gropelli, G., Viereck-Goette, L., eds., Stratigraphy and Geology of Volcanic Areas: Geological Society of America Special Paper 464, p. 1-32.

Nomade, S., Renne, P.R., Vogel N., Deino, A.L., Sharp, W.D., Becker, T.A., Jaouni, A.R., Mundil, R., 2007. Alder Creek sanidine (ACs-2): A Quaternary 40Ar/39Ar dating standard tied to the Cobb Mountain geomagnetic event 218, 315-338.

Olson, P.I., Coe, R.S., Driscoll, P.E., and Glatzmaier, G.A., Roberts, P.H., 2010. Geodynamo reversal frequency and heterogeneous core-mantle boundary heat flow. Phys. Earth Planet. Inter. 180, 66-79.

Osete, M-L., Martin-Chivelet, J., Rossi, C., Edwards, R.L., Egli, R., Munoz-Garcia, M.B., Wang, X., Pavon-Carrasco, J., Heller, F., 2012. The Blake geomagnetic excursion recorded in a radiometrically dated speleothem. Earth Planet. Sci. Lett. 353-354, 173-181.

Renne, P.R., Swisher, C.C., Deino, A.L., Karner, D.B., Owens, T.L., DePaolo, D.J., 1998. Intercalibration of standards, absolute ages and uncertainties in 40Ar/39Ar dating, Chem. Geol. 145, 117-152.

Roberts, A.P., 2008. Geomagnetic excursions: knowns and unknowns. Geophys. Res. Lett., 35, L17307, doi: 10.1029/2008GL034719.

Scaillet, S., Guillou, H., 2004. A critical evaluation of young (near zero) K-Ar Ages. Earth Planet. Sci. Lett., 220, 265-275.

Singer, B.S., Hoffman, K.A., Chauvin, A., Coe, R.S., Pringle, M.S., 1999. Dating transitionally magnetized lavas of the late Matuyama chron: Toward a new 40Ar/39Ar timescale of reversals and events. J. Geophys. Res. 104, 679-693.

Singer, B.S., Relle, M.R., Hoffman, K.A., Battle, A., Guillou, H., Laj, C., Carracedo, J.C., 2002.

Ar/Ar ages of transitionally magnetized lavas on La Palma, Canary Islands, and the Geomagnetic Instability Timescale. J. Geophys. Res. 107, 2307, doi:10.1029/2001JB001613.

Singer, B.S., Brown, L., Rabassa, J., Guillou, H., 2004a. 40Ar/39Ar chronology of late Pliocene and Early Pleistocene geomagnetic and glacial events in southern Argentina. in: Timescales of the Paleomagnetic Field, J.E.T. Channell et al. (eds.), AGU Geophysical Monograph 145, pp. 175-190.

Singer, B.S., Ackert, R.P., Guillou, H., 2004b. 40Ar/39Ar and K-Ar chronology of Pleistocene glaciations in Patagonia. Geol. Soc. Am. Bull. 116, 434-450.

Singer, B.S., Jicha, B.R., Kirby, B.T., Geissman, J.W, Herrero-Bervera, E., 2008a. 40Ar/39Ar dating links Albuquerque Volcanoes to the Pringle Falls excursion and the Geomagnetic Instability Time Scale. Earth Planet. Sci. Lett. 267, 584-595.

Singer, B.S., Hoffman, K.A., Schnepp, E., Guillou, H., 2008b. Multiple Brunhes Chron Excursions in the West Eifel Volcanic Field: Support for long-held mantle control on the non-axial dipole field. Phys. Earth Planet. Inter. 169, 28-40.

Singer, BS, Guillou, H., Jicha, BR., Laj, C., Kissel, C., Beard, BL., Johnson, CM., 2009. 40Ar/39Ar, K-Ar and 230Th-238U dating of the Laschamp excursion: A radioisotopic tie-point for ice core and climate chronologies. Earth Planet. Sci. Lett. 286, 80-88.

Singer, B.S., Jicha, B.R., He, H., Zhu, R., 2011. 40Ar/39Ar evidence for a 17 ka geomagnetic field excursion at Changbaishan volcano, northeastern China. EOS, Transactions of the American Geophysical Union abstract, GP13A-04.

Singer, B.S., 2007. Polarity Transitions: Radioisotopic Dating. In: Gubbins, D., and Herrero-Bervera, E., eds. Encyclopedia of Geomagnetism and Paleomagnetism. Springer, pp. 834-839.

Singer, B.S., Jicha, B.R., Coe R.S., Mochizuki, N., 2012. An EARTHTIME chronology for the Matuyama-Brunhes reversal. EOS, Transactions of the American Geophysical Union abstract, V21E-06.

Smith, J.D., Foster, J.H., 1969. Geomagnetic reversal in the Brunhes normal polarity epoch. Science 163, 565-567.

Spell, T.L., McDougall, I., 2003. Characterization and calibration of 40Ar/39Ar dating standards, Chem. Geol., 198, 189-211.

Thouveny,N., K.M. Creer, K.M., Blunk, I., 1990. Extension of the Lac du Bouchet palaeomagnetic record over the last 120,000 years. Earth Planet. Sci. Lett. 97, 140-161.

Thouveny, N., Carcaillet, J,. Moreno, E., Leduc, G., Nérini, D., 2004. Geomagnetic moment variation and paleomagnetic excursions since 400 kyr BP: a stacked record from sedimentary sequences of the Portugese margin. Earth Planet. Sci. Lett. 219, 377-396.

Tric, E., Laj, C., Valet, J-P., Tucholka, P., Paterne, M., Guichard, F., 1991. The Blake geomagnetic event: transition geometry, dynamical characteristics and geomagnetic significance. Earth Planet. Sci. Lett. 102, 1-13.

Tucholka, P., Fontugne, M., Guichard, F., Paterne, M., 1987. The Blake polarity episode in cores from the Mediterranean Sea. Earth Planet. Sci. Lett. 86, 320-326.

Turner G.M., Lyons R.G., 1986. A paleomagnetic secular variation record from c. 120000 yr-old New Zealand cave sediments. Geophysical Journal of the Royal Astronomical Society, 87, 1181-1192.

Valet, J.P., Meynadier L., Guyodo, Y., 2005. Geomagnetic field strength and reversal rate over the past 2 Million years. Nature 435, 802-805.

Zanella, E, Laurenzi, M.A., 1998. Evidence for the Blake event in volcanic rocks from Lipari (Aeolian Archipelago). Geophys. J. Int. 132, 149-158.

Zhang, K., Gubbins, D., 2000, Is the geodynamo process intrinsically unstable? Geophys. J. Int. 140, F1-F4.

Zhu, R.X., Zhou, L.P., Laj, C., Mazaud, A., Ding, D.L., 1994. The Blake geomagnetic polarity episode recorded in Chinese loess. Geophys. Res. Lett. 21, 697-700.

Zhu, R., Pan, Y, Coe, R.S., 2000. Paleointensity studies of a lava succession from Jilin Province, northeastern China: Evidence for the Blake event. J. Geophys. Res. 105, 8305-8317.

Tables & Figure captions

Table 1. List of records documenting the Blake excursion.

Table 2. Results of unspiked K-Ar experiments on Lipari Island samples.

Table 3. Summary of 40Ar/39Ar results from Lipari and Amsterdam Islands and the El Calderon basalt flow, New Mexico.

Figure 1. Map of Lipari Island highlighting the Lo Inzolfato lava flow and sites of samples LP-06-01, -02, -03, -04, and -05. Digital Elevation map and distribution of the Lo Inzolfato lava (with younger pyroclastic rocks that cover parts of the flow removed) from Lucchi et al. (2010).

Figure 2. Topographic map of Amsterdam Island, highlighting the location of lava flow samples Am-1, -2, -3, and -4 from which paleodirectional and paleointensity data were collected by Carvallo et al. (2003). Redrawn from Carvallo et al. (2003).

Figure 3. Age spectra and isochron diagrams for lava flow samples from Lipari and Amsterdam Island and the El Calderon basalt flow, New Mexico. Note the two sets of experients on Lipari sample LP-06-03 from UW-Madison and Gif-sur-Yvette give identical results.

Figure 4. Virtual Geomagnetic Pole (VGP) plot for Blake and Post-Blake sediment and lava records. Red path connects VGPs observed in sediment from the eastern Mediterranean Sea that include two loops into southern South America, with the latter loop punctuated by the transit and clustering over Australasia (data from Tric et al., 1991; Figure adapted from Laj and Channell, 2007). VGPs from the 40Ar/39Ar-dated lava flows on Lipari (Zanella and Laurenzi, 1999) and Amsterdam (Carvallo et al., 2003) Islands and the El Calderon lava flow, New Mexico (Champion et al., 1988; Cascadden, 1997) are plotted.

Figure 5. The Geomagnetic Instability Time Scale (GITS) for the Brunhes chron. For comparison, column at left shows the seven well-dated excursions summarized by Laj and Channell (2007), the inclination records are a composite from North Atlantic sediment at ODP sites 919, 983, and 984 (Channell, 1999, 2006; Channell et al., 2004), SINT-2000 paleointensity stack is from Valet et al. (2005), and PISO-1500 paleointensity stack from Channell et al. (2009). Vertical dashed line in the PISO-1500 stack at 3x1022 Am2 is an indicator of low paleointensity (see text for discussion). Ages in the GITS are from 40Ar/39Ar-dated lava flows with exception of the Iceland Basin and Stage 17 excursions that are astrochronologically-dated in ODP cores (Channell, 2006, Channell et al., 2004). The 40Ar/39Ar ages used in the GITS are calculated or re-calculated relative to 28.201 Ma Fish Canyon sanidine (Kuiper et al., 2008), but see Singer et al. (2012) for potential problems with this simple approach to re-calculating many of these ages. It is important to note that regardless of whether we use the more traditional 28.02 Ma age for the FCs standard (and a 40K decay constant of 5.543×10^{-10}/y), or the astrochronologically calibrated values of Kuiper et al. (2008), neither the number of Brunhes chron excursions, nor the durations of the intervals separating them in time, are affected.

Table 1

Ref.[a]	Location	Age (ka)	Duration (ka)	MIS	Method	Comments
Blake excursion						
Sediments						
1	Blake Rise	114 – 108	5–7		Foraminifera, sedimentation rate	10% uncertainty in age
2	Greater Antilles Ridge	Uncertain			Microfossils	
3	Tauro, Italy	155 – 105	50		Sedimentation rate, microfossils	Two reversed intervals 16 and 23 ka long
4	Central Mediterranean	118 – 114	8	5d-e	Oxygen isotopes of foraminifera	
4,5	Eastern Mediterranean	118 – 112	4.5	5d-e	Oxygen isotopes of foraminifera	Two reversed intervals
6,7	Portugese margin	122 – 115		5d-e	Oxygen isotopes, 10Be spike	Associated with low intensity and ^{10}Be spike
8	Lac du Bouchet, France	117	10?		Pollen-MIS correlation	End of inclination anomaly
Cave deposits						
9	North Island, New Zealand	120 ± 6			U-Th disequilibrium on flowstone	Pre-Blake weakening of dipole field?
10	Cobre Cave, Spain stalagmite	116.5 – 112.0	4.5		^{230}Th on speleothem	2 periods of reversed polarity
Lava flows						
11	Laguna Basalt flow, New Mexico	128 ± 66			K-Ar dating, whole rock	
12	Laguna Basalt flow, New Mexico	54 ± 100			K-Ar dating, whole rock	
13	Lipari (Aeolian Archipeligo), Italy	128 ± 46			^{40}Ar/^{39}Ar incremental heating	Strongly discordant age spectra
14	Changbaishan Volcano, China	123 ± 14			^{40}Ar/^{39}Ar incremental heating	Data not reported, standard uncalibrated
post-Blake excursion						
8	Lac du Bouchet, France	104, 95	1 each	5c	Pollen-MIS correlation	2 inclination anomalies
6,7	Portugese margin	105 – 95		5c	Oxygen isotopes, MIS correlation	Defined by low intensity and ^{10}Be spike
15	Skalamaelifell lava flows, Iceland	94 ± 8			^{40}Ar/^{39}Ar and ^{238}U/^{230}Th dating	Originally interpreted as Laschamp excursion

[a] References: (1) Smith and Foster (1969); (2) Denham (1976); (3) Creer et al. (1980); (4) Tucholka et al. (1987); (5) Tric et al. (1991); (6) Thouveny et al. (2004); (7) Carcaillet et al. (2004); (8) Thouveny et al. (1990); (9) Turner and Lyons (1986); (10) Osete et al. (2012); (11) Champion et al. (1988); (12) Laughlin et al. (1993); (13) Zanella and Laurenzi (1998); (14) Zhu et al. (2000); (15) Jicha et al. (2011).

Table 2

Sample ID Experiment n°	Weight molten (g)	K* (wt.%)	$^{40}Ar^*$ (%)	$^{40}Ar^*$ (10^{-13} mol/g)	$^{40}Ar^*$ weighted mean ($\pm 1\sigma$)	Age $\pm 2\sigma$ ka
LP06-02						
7824	0.95469	3.885 ± 0.039	3.124	7.002		103.9 ± 4.8
LP-06-03						
7823	1.11568	3.744 ± 0.037	1.773	6.490		
7839	1.26967	"............"	3.958	6.752	6.637 ± 0.086	102.2 ± 3.4
LP-06-04						
7353	1.26789	3.678 ± 0.037	2.251	6.389		
7369	1.21287	"............"	3.112	5.963	6.177 ± 0.078	96.8 ± 3.1
LP-06-05						
7290	1.22341	3.752 ± 0.037	1.569	6.405		
7322	1.31719	"............"	1.503	6.253	6.321 ± 0.066	97.1 ± 2.8

Table 3

Sample #	Lat	Long	K/Ca total	Total fusion Age (Ma) ± 2σ	$^{40}Ar/^{36}Ar_1$ ± 2σ	MSWD	Isochron Age (ka) ± 2σ	N	^{39}Ar %	MSWD	Plateau Age (ka) ± 2σ
Lipari											
LP-06-03	38.50439	14.90872	1.27	103.5 ± 5.2	295.6 ± 4.8	0.54	103.0 ± 7.6	10 of 10	100.0	0.48	103.1 ± 4.7
			1.27	109.1 ± 5.4	295.7 ± 5.8	2.18	106.0 ± 9.9	10 of 10	100.0	1.94	106.3 ± 5.6
			1.12	108.3 ± 5.1	298.9 ± 3.3	0.98	103.0 ± 6.6	10 of 10	100.0	1.33	107.3 ± 4.5
			1.34	107.5 ± 4.6	294.5 ± 3.8	1.30	108.3 ± 7.1	10 of 10	100.0	1.19	106.9 ± 4.5
Weighted mean plateau age from 4 experiments:											**105.9 ± 2.1**
LP-06-03[a]	38.50439	14.90872	0.99	104.1 ± 2.8	295.5 ± 2.2	0.29	104.1 ± 4.2	8 of 8	100.0	0.25	104.0 ± 2.3
			1.33	105.5 ± 2.9	295.0 ± 2.7	0.56	106.6 ± 5.4	8 of 8	100.0	0.51	105.8 ± 2.6
Weighted mean plateau age from 2 experiments:											**104.8 ± 1.7**
LP-06-04	38.50292	14.92160	1.49	118.7 ± 9.9	No isochron			10		4.79	No plateau
			1.83	128.7 ± 10.6	No isochron			11		6.25	No plateau
			0.64	197.8 ± 20.6	No isochron			8		4.65	No plateau
LP-06-05	38.50372	14.90940	1.52	109.3 ± 13.0	296.1 ± 4.7	0.27	79.3 ± 38.5	5 of 11	54.3	0.21	84.1 ± 7.5
			1.32	162.0 ± 14.2	No isochron			11		20.33	No plateau
			0.97	197.8 ± 20.6	No isochron			8		17.83	No plateau
El Calderon flow, New Mexico											
NM-10-02	35.07476	−107.755527	0.13	111.6 ± 41.1	296.8 ± 3.1	0.42	60.5 ± 63.6	8 of 9	98.8	0.46	107.4 ± 35.9
			0.11	119.5 ± 56.8	294.4 ± 4.2	0.26	167.5 ± 129.8	8 of 8	100.0	0.27	128.6 ± 42.7
			0.11	103.5 ± 52.9	296.9 ± 4.0	0.82	51.4 ± 47.6	7 of 7	100.0	0.77	99.3 ± 44.6
Weighted mean plateau age from 3 experiments:											**112 ± 23**
NM-10-03	35.09521	−107.78517	0.12	126.2 ± 42.0	296.6 ± 3.1	0.58	85.6 ± 50.4	9 of 9	100.0	0.58	106.8 ± 26.9
			0.11	108.3 ± 41.6	297.2 ± 2.3	0.53	62.8 ± 43.8	7 of 7	100.0	0.82	96.2 ± 29.3
			0.12	104.3 ± 33.4	296.0 ± 3.9	0.14	92.3 ± 50.5	7 of 7	100.0	0.13	99.0 ± 20.6
Weighted mean plateau age from 3 experiments:											**101 ± 14**
Amsterdam Island											
Am-2	−37.8049	77.53149	0.07	132.9 ± 30.5	296.0 ± 1.0	0.24	100.4 ± 50.4	6 of 6	100.0	0.39	122.9 ± 25.6
			0.07	105.2 ± 52.8	295.7 ± 1.2	0.10	97.8 ± 54.5	7 of 8	99.9	0.10	106.2 ± 27.9
			0.07	155.3 ± 42.1	296.5 ± 1.5	0.20	102.2 ± 56.5	7 of 7	100.0	0.48	135.9 ± 32.1
			0.09	108.5 ± 42.3	295.6 ± 1.1	0.53	111.9 ± 48.3	6 of 7	99.7	0.43	115.9 ± 28.5
			0.08	107.5 ± 30.2	295.0 ± 1.3	0.13	138.3 ± 43.8	6 of 7	90.2	0.23	124.0 ± 26.2
Weighted mean plateau age from 5 experiments:											**120 ± 12**

Ages calculated relative to 28.201 Ma Fish Canyon sanidine, or a standard intercalibrated to this value. Age in **bold** is preferred.

[a] Experiments at Gif-sur-Yvette, France, all others at UW-Madison.
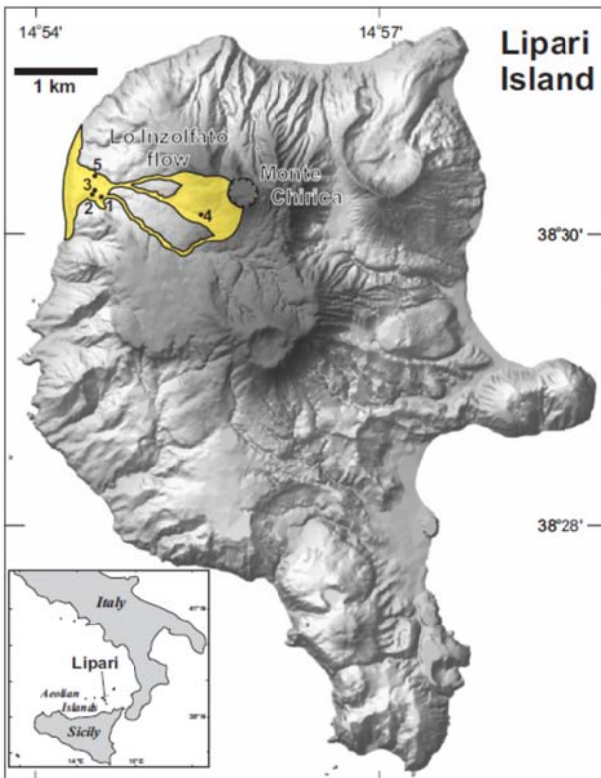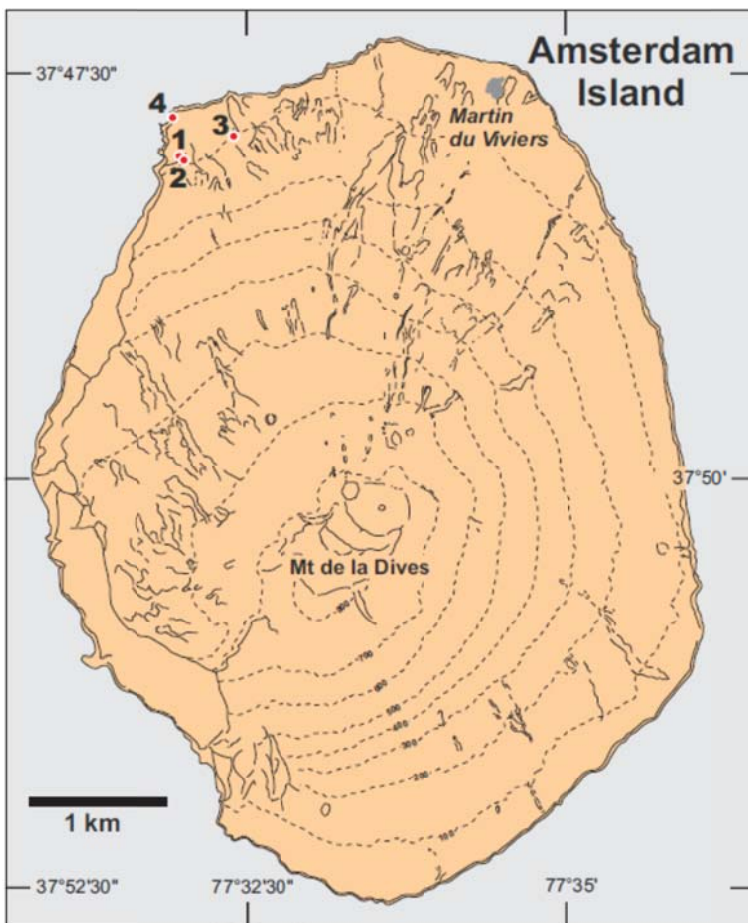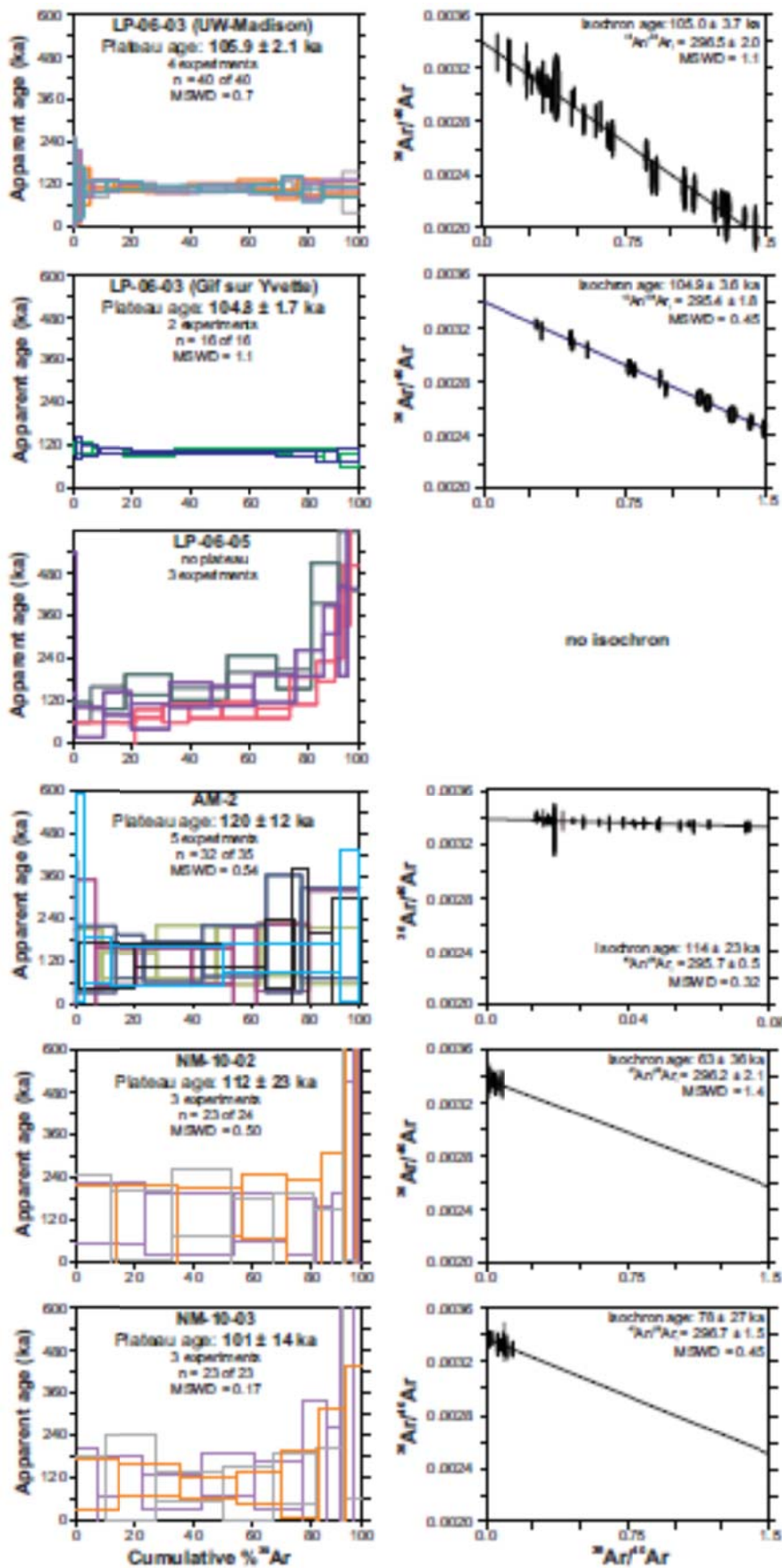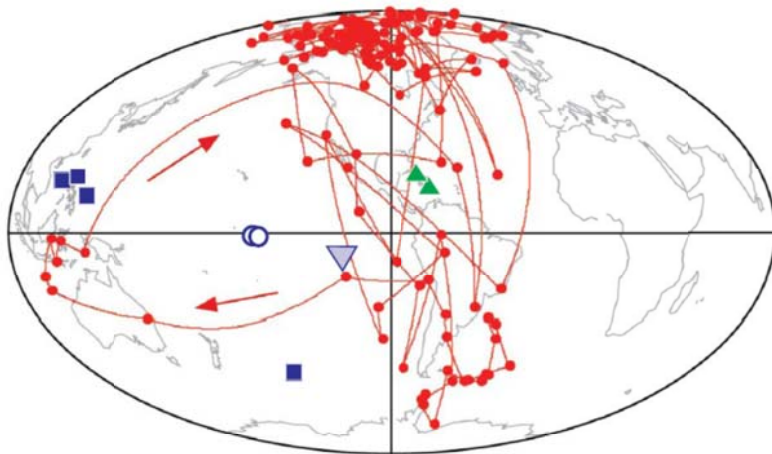
Figure 1

Figure 2

Figure 3

Figure 4

118 - 114 ka   Tric et al. (1991) Mediterranean sed.
105 ± 1 ka   ■ Lipari
104 ± 12 ka ○ El Calderon, NM
120 ± 12 ka ▲ Amsterdam
94 ± 8 ka   ▽ Skalamaelifell, Iceland

Figure 5